Materials Today Advances 12 (2021) 100187

Contents lists available at ScienceDirect

Materials Today Advances

journal homepage: www.journals.elsevier.com/materials-today-advances/

Surface nanotopography mediated albumin adsorption, unfolding and modulation of early innate immune responses

Panthihage Ruvini L. Dabare [a, 1], Akash Bachhuka [a, b, **, 1], Emma Parkinson-Lawrence [c], Krasimir Vasilev [a, *]

[a] UniSA STEM, University of South Australia, Mawson Lakes, South Australia, 5095, Australia
[b] Department of Electronics, Electric and Automatic Engineering, Rovira i Virgili University (URV), Tarragona, 43003, Spain
[c] Mechanisms in Cell Biology and Diseases Research Group, UniSA Clinical and Health Sciences. University of South Australia, City East Campus, Adelaide, 5000, Australia

ARTICLE INFO

Article history:
Received 29 September 2021
Received in revised form
18 November 2021
Accepted 22 November 2021
Available online 26 November 2021

Keywords:
Plasma polymerization
Nanotopography
Albumin adsorption
Immune cells interaction
Immune response

ABSTRACT

Surface roughness plays an important role in regulating protein adsorption to biomaterial surfaces and modulating the subsequent inflammatory response. In this study, we examined the role of surface nanotopography on albumin adsorption, unfolding and subsequent immune responses. To achieve the objectives of the study, we create model surfaces of hill-like nanoprotrusions by covalently immobilizing gold nanoparticles (AuNPs) of predetermined sizes (16, 38, and 68 nm) on a functional plasma polymer layer. The amount of adsorbed albumin increased with the increase in surface area caused by greater surface nanotopography scales. Circular dichroism spectroscopy was used to evaluate albumin conformational changes and pointed to loss of α-helical structure on all model surfaces with the greatest conformational changes found on the smooth surface and the surface with largest nanotopography features. Studies with differentiated THP-1 cells (dTHP-1) demonstrated that immune cells interacted with surface adsorbed albumin via their scavenger receptors, which could bind to exposed peptide sequences caused by surface induced unfolding of the albumin. Pre-adsorption of albumin resulted in an overall decrease in the level of expression of pro-inflammatory cytokines from dTHP-1 cells. On the other hand, pre-adsorption of albumin led in an increase in the production of anti-inflammatory markers, which suggests a switch to the M2 pro-healing phenotype. The knowledge obtained from this study could instruct the design of healthcare materials where the generation of targeted surface nanotopography and pre-adsorption of albumin may enhance the biomaterial biocompatibility and lead to faster wound healing.

1. Introduction

Biomaterials are an integral part of current healthcare services spanning from implantation to diagnostics and imaging. However, their performance can be compromised by innate inflammatory responses resulting from a foreign body reaction (FBR). The inflammation induced by FBR process is initiated by the adsorption of nonspecific serum proteins onto the surface of the biomaterial. The interplay of protein adsorption and desorption then governs the subsequent immune responses i.e. immune cell-surface interaction, cell-cell interaction, cytokines release, and ultimately the fibrous capsule formation leading to plaque formation and implant failure [1–3] (Scheme 1).

The amount, type, and conformation of adsorbed proteins are known to be dependent on the surface features of the biomaterials such as topography, roughness, chemistry, energy, and wettability [2,5–9]. Some key serum proteins known to adsorb rapidly onto the surface of biomaterials include fibrinogen, fibronectin, albumin, vitronectin, immunoglobulins, and complement protein [4,10]. The amount and type of the adsorbed proteins modulate immune cell adhesion through various receptors, directing their fate either towards pro-inflammatory or anti-inflammatory phenotypes. In the last decade, much research has focused on interrogating protein

* Corresponding author.
** Corresponding author. UniSA STEM, University of South Australia, Mawson Lakes, South Australia, 5095, Australia.
E-mail addresses: akash.bachhuka@urv.cat (A. Bachhuka), Krasimir.vasilev@unisa.edu.au (K. Vasilev).
[1] Equal first author.

https://doi.org/10.1016/j.mtadv.2021.100187

Abbreviations

AFM	Atomic Force Microscope/Microscopy
ANOVA	one-way analysis of variance
AuNPs	gold nanoparticles
CDS	Circular dichroism spectroscopy
dTHP-1	differentiated THP-1
eV	Electron volt
FBR	foreign body reaction
FBS	fetal bovine serum
h	hours
HSA	Human serum albumin
min	minutes
nm	nanometre(s)
PBS	phosphate buffer saline
PI	polyinosinic acid
PMA	phorbol 12-myristate 13-acetate
pOX	2-methyl-2- oxazoline
RMS	Root Mean Square roughness
RPMI	Roswell Park Memorial Institute
SEM	Standard error mean
SR-AI	scavenger receptor AI
s	seconds
XPS	X-ray photoelectron spectroscopy

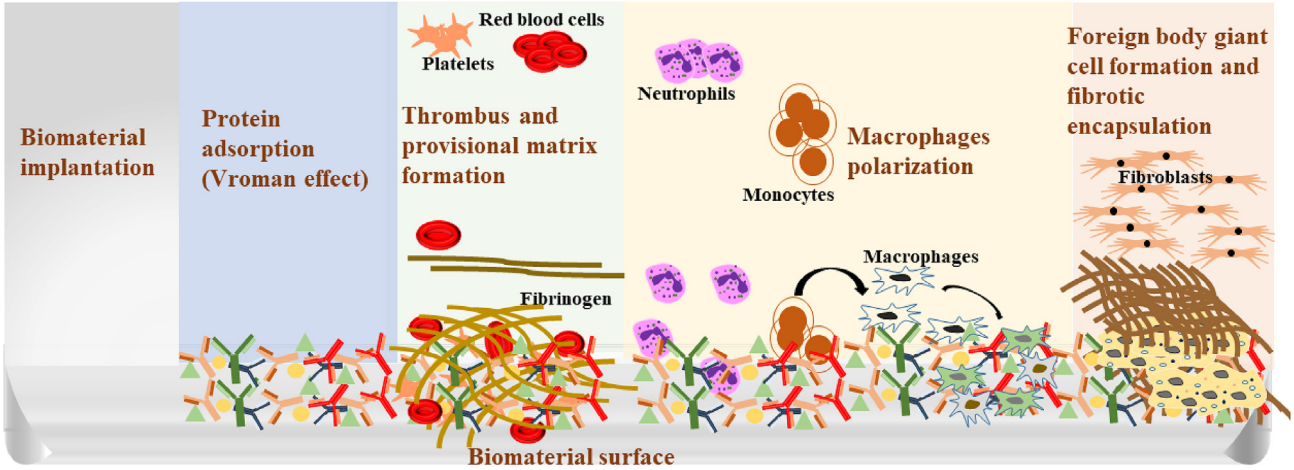

Scheme 1. Cascade of foreign body reaction on biomaterial surface. adapted from Christo et al. [4].

unfolding at surface interphases, as it is now known to significantly alter interactions between the biomaterial and immune cells. Visalakshan et al. demonstrated that unfolding of fibrinogen leads to the exposure of a hidden receptor which binds to Mac-1 integrin receptors of monocytes to induce proinflammatory response [11]. Shen et al. revealed that different surface chemistry can lead to the adsorption of different amount of proteins such as fibrinogen, fibronectin, IgG, and albumin, further modulating monocytes adhesion [12]. A study by Keselowsky et al. showed that fibronectin can modulate the formation of foreign body giant cells on the surface of biomaterials [13].

Albumin is an essential serum protein known to play a dominant role in FBR as it is one of the major proteins in the protein corona formed on the surface of a biomaterial [14]. The high level of albumin in the protein corona is due to its low molecular weight (68 KDa) and its abundance in the blood (40 mg/mL) [3,5,15]. Albumin is a 585 amino acid globular protein, folded into three structurally similar domains (1,2 and 3) resembling heart shape. Each of these domains consists of two subdomains (A, B) [15] (Scheme 2). Furthermore, it exists in 3 different forms based on the pH of the medium i.e. *N*-form (4.3–8.0), F-form (pH < 4.3), and B-form (pH > 8) [3]. Albumin has also been reported to regulate osmotic pressure and has been used as a carrier for drugs and fatty acids [16,17]. It has also been used as a coat on implantable and sensing devices to prevent platelet coagulation, adhesion of other proteins, cells, and bacteria [2,18–21].

Given the importance of albumin in physiological processes and its abundance in biological fluids, it is of paramount importance to understand the interactions of albumin with biomaterials. The effect of adsorbed albumin on nanoparticle clearance has been investigated in several studies [22,23]. Santos et al. reported that an albumin bath can reduce the uptake of mesoporous silica nanoparticles from the mononuclear phagocyte system [23]. Absorption onto nanoparticles can also lead to structural changes in albumin molecules which then allows the binding of macrophages via scavenger receptor AI (SR-AI) [15]. Albumin adsorption has also been extensively studied to interrogate the influence of biomaterials surface chemistry [2,14,24]. However, much less is known about the effect of surface nanotopography on albumin adsorption and conformational changes, and how these may affect the subsequent immunological responses.

To shed light on these events, we created model substrata having well-defined surface characteristics in terms of nanotopography and outermost surface chemistry. To generate surface hill-like nanoprotrusions of targeted dimensions at the nanoscale, we used gold nanoparticles (AuNPs) of diameters of 16, 38, and 68 nm which we covalently immobilized in equal number density to functional oxazoline based plasma polymer coating. In the next step, we established uniform outermost surface chemistry by applying a 5 nm thin plasma polymer coating deposited from vapor of 2-methyl-2-oxazoline (pOX). These model substrata were then utilized to interrogate albumin adsorption and conformational changes, and how these modulated the early innate immune responses in cultured monocytes and macrophages.

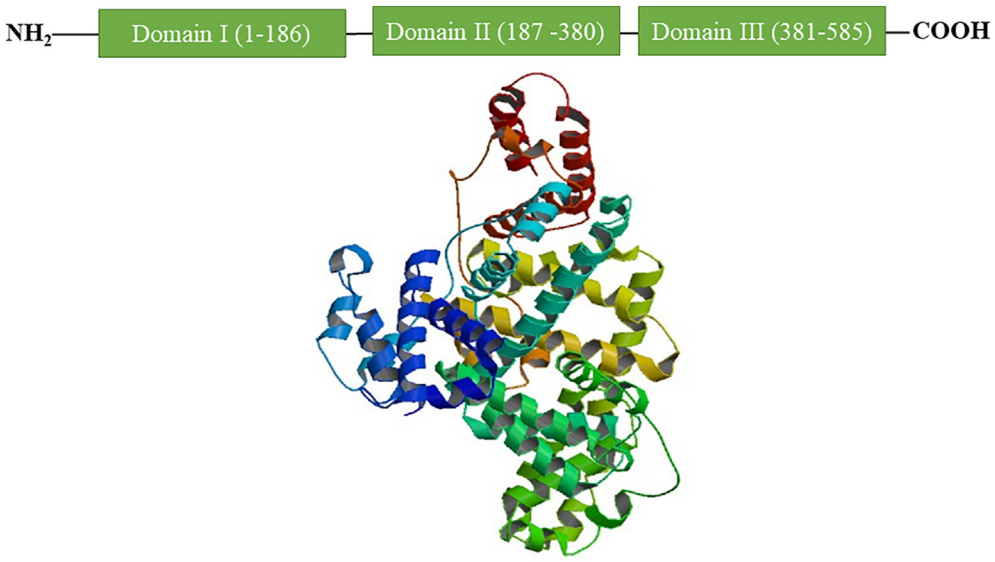

Scheme 2. Structure of the albumin molecule. (Acquired from protein data bank – RCSB PDB: 1E78).

2. Experimental methods

2.1. Materials

Unless otherwise specified, chemicals, THP-1 cells, albumin, and culture media used in the experiments were purchased from Sigma-Aldrich (Merck Group) and used as received.

2.2. Surface preparation

2.2.1. Plasma polymerization

Plasma polymerization was used to coat a 20 nm layer of 2-methyl-2-oxazoline (pOX) on model substrates. A custom-built plasma reactor equipped with 13.56 MHz plasma generator, described elsewhere was used to perform the plasma polymerization process [25]. Model substrates such as glass coverslips, silicon wafers, quartz glasses, and tissue culture plates were cleaned with ethanol and acetone followed by air cleaning for 5 min at the radio power of 50 W and pressure of 0.1 mbar. After air cleaning, surfaces were coated with pOX at the pressure of 0.08 mbar, 50 W radio power for 2 min (Scheme 3) [26].

2.2.2. Gold nanoparticles (AuNPs) synthesis and surface immobilization

The AuNPs were synthesized by citrate reduction of gold chloride [27]. Briefly, 50 μL of gold (III) chloride trihydrate (100 mg/mL) was added to 50 mL of Milli-Q water. The solution was heated in a controlled reflux system at 150 °C and 1300 rpm. 1% trisodium citrate was added to the boiling solution in different concentrations (1, 0.5, and 0.3 mL) to produce AuNP of diameters of 16 nm, 38 nm and 68 nm, respectively. After adding trisodium citrate, the solution was heated for another 20 min. The heating source was removed but the solution was further stirred at 1300 rpm until cool. Mercaptosuccinic acid (1.5 mg/mL) along with sodium hydroxide (0.81 mg/mL) was added to the AuNPs solution. Finally, the solution was stirred at 300 rpm for 8–12 h to cap the nanoparticles with carboxylic acid functional groups.

For surface immobilization, pOX coated substrates were immersed in the AuNPs suspension synthesized as described above. Different parameters such as pH, concentration of the AuNP suspension and time of immersion were utilized to obtain well-defined nanotopography (equal number of nanoparticles per unit area). The pH of the suspension was maintained at 4 for all AuNPs. For 16 nm AuNPs, a 1:10 dilution was prepared using Milli-Q water and surfaces were immersed in this solution for 1 h and 10 min. Furthermore, plasma polymerized surfaces were immersed in 38 and 68 nm AuNPs for 1 h and 20 min and 5 h, respectively, without any dilution [11,26]. The surfaces were washed thrice with Milli-Q water to remove any unbound nanoparticles and were dried using N_2 gas flow.

2.2.3. Surface overcoating

Nanotopography modified surfaces were coated with a thin layer of pOX (~5 nm) using the plasma polymer deposition system described above using the pressure of 0.08 mbar and power of 50 W for 25 s. These conditions allow preserving the scale of nanotopography while achieving uniform outermost surface chemistry.

2.3. Characterization of the model substrata

2.3.1. Surface nanotopography

Atomic Force Microscopy (AFM) was used to analyze the surface morphology of the model substrata. Imaging of the surface was conducted using the NT-MDT NTEGRA SPM AFM instrument in non-contact mode. Gold coated silicon nitride non-contact cantilever (NT-MDT, NSG03) with resonance frequencies between 65 and 100 kHz was used. The oscillation amplitude was 10 nm. To obtain 5 μm × 5 μm images a scan rate of 0.5 Hz was used. Images were analysed using and Gwyddion software [28].

2.3.2. Chemical analysis - X-Ray Photoelectron Spectroscopy

X-ray Photoelectron Spectroscopy (XPS) was performed to determine the surface chemistry of the model surfaces. A SPECS SAGE XPS system with a Phoibos 150 hemispherical analyzer and MCD-9 detector was used. All results were obtained using a non-monochromated MgKα radiation source (hν: 1253.6 eV) operated at 10 kV and 20 mA (200 W). Survey spectra from 0 to 1000 eV were performed at 100 eV pass energy with 0.5 eV resolution. High-resolution scans were conducted for C, N, O, and Au to quantify the concentration of these elements present at the surface. Casa XPS software (http://www.casaxps.com/) was used for analysis.

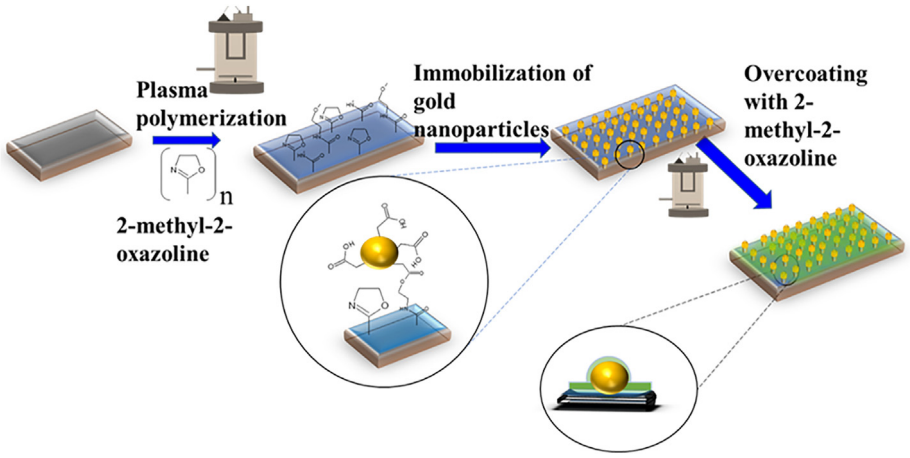

Scheme 3. Schematic representation of the process utilized to generate model surfaces having controlled hill-like nanotopography and uniform outermost surface chemistry.

2.3.3. Plasma polymer film thickness

The thickness of the pOX coating was measured using the J. A. Woolam Co. variable angle spectroscopic ellipsometer (VASE). Data were analysed using WVASE32 software (J. A. Woolam). For ellipsometry measurements, coatings were deposited on silicon wafers.

2.3.4. Wettability of surfaces

Surface wettability was determined by measuring the angle of a static water droplet at the solid/liquid/gas air interface. RD-SDM02 contact angle measuring equipment was used for acquiring images of the water droplet. All images were analysed using ImageJ software.

2.4. Quantification of adsorbed albumin

2.4.1. Micro BCA method

The amount of albumin adsorbed onto model surfaces was determined by Micro BCA (Thermo Fischer Scientific, Life Technologies Australia).12 well tissue culture plates with a surface area of 3.8 cm^2 (Corning®) were modified with the targeted surface nanotopography and chemistry [11]. Firstly, the wells of the plates were thoroughly washed with phosphate buffer saline (PBS). Human serum albumin (HSA) (1 mg/mL) solution was incubated with model surfaces for 1 h at room temperature followed by three times washing with PBS to remove any unbound albumin. BCA working reagent was prepared as per the manufacturer's instructions. Surfaces were incubated with 250 μL of BCA working reagent for 2 h at 37 °C. After incubation, 200 μL solution was taken out and was added into a 96 well tissue culture plate. Absorbance was measured at 562 nm using a plate reader (FLUOstar Optima, BMG Labtech). The amount of HSA adsorption was determined by fitting the absorbance value in the standard curve obtained for HSA.

2.5. Circular dichroism spectroscopy (CDS)

CDS is used to determine the conformational changes of protein including unfolding of α and β sheets and tertiary structure. CDS was performed on the modified surfaces using established protocols [11]. Desired surface modification was applied to a quartz slide (40 × 9.5 × 1 mm) and incubated in 1 mg/mL HSA solution for 1 h at ambient temperature followed by washing with PBS to remove any unbound HSA. CD spectra were obtained in the range of 200 nm−260 nm with a resolution of 0.2 nm, 1 nm bandwidth, and a scanning speed 50 nm min^{-1}. Eight accumulations of CD spectra were recorded before and after HSA adsorption for each sample to reduce the signal-to-noise ratio. A baseline corrected spectrum of 1 mg/mL HSA was obtained for native albumin.

Raw data (millidegrees) was expressed as molar residue ellipticity (MRE) using the Dichoweb CD analysis software. The K2D method was used to determine the amount of secondary structure in absorbed albumin using Dichroweb software [29–31].

2.6. Cell cultures

THP-1 human monocytic cells were obtained from Sigma Aldrich-Merck group. Cells were cultured in Roswell Park Memorial Institute (RPMI) 1640 media supplemented with 10% v/v fetal bovine serum (FBS, gibco, Life Technologies Australia) and 1% v/v penicillin and streptomycin (gibco, Life Technologies USA). Cell cultures were incubated at 37 °C in 5% CO_2 air. Cell density was maintained between 1×10^5 and 1×10^6 viable cells/mL.

2.7. Immune cells interaction with HSA

The THP-1 monocytes and macrophages differentiated from THP-1 (dTHP-1) were used for determining the interaction of cells with surface adsorbed albumin. THP-1 monocytes were stimulated with 100 ng/mL phorbol 12-myristate 13-acetate (PMA) in RPMI media for 48 h followed by changing with PMA free media for 24 h to obtain dTHP-1 macrophages [32]. Nanotopography and chemistry modified tissue culture well plates were precoated with HSA using 1 mg/mL for 1 h. Monocytes and macrophages at 1×10^5 viable cells/mL were used for this experiment. Cells were incubated with modified surfaces with and without adsorbed albumin for 1 h at 37 °C in 5% CO_2 air. A shorter period was used for this assay to differentiate cell attachment by unstimulated cells and to minimize the effect from nutrient lack serum free medium. The media was removed, and surfaces washed three times with PBS to remove any unbound cells. Cells were stained with fluorescent live-cell tracker, NucBlue™ dye (Thermo Fisher Scientific, Australia) for 15 min, and visualized using fluorescence microscopy (Olympus IX83) [11].

2.8. Selective binding with scavenger receptors

Native albumin does not express the epitopes for binding to scavenger receptors of macrophages. Albumin needs to undergo structural modifications to expose ligands for scavenger receptors [15]. To confirm the effect of surface properties on the conformation of albumin, polyinosinic acid (PI) was used. Polyinosinic acid

selectively binds with scavenger receptors (SR-A1) of macrophages and blocks the interaction of cells and albumin. dTHP-1 cells at 1×10^4 cells/mL were incubated with PI (100 μg/mL) for 1 h and seeded onto surfaces with and without albumin. The pre-treated cells were incubated on the modified surfaces for 1 h at 37 °C in 5% CO_2 atmosphere. The media was removed, and the surfaces were washed with PBS to remove any unbound cells. NucBlue™ was used to visualize the surfaces under the fluorescence microscope.

2.9. Immune response

The immune response from monocytes and macrophages was determined by using 24 tissue culture well plates with modified surfaces. The modified surfaces were incubated with 1 mg/mL of HSA in PBS for 1 h followed by washing with PBS. Cell seeding density was maintained at 1×10^5 cells/mL. Serum-free RPMI media was used throughout this experiment to distinguish the effect of albumin. Cells were seeded onto the modified surface with and without albumin and incubated for 2 h at 37 °C in 5% CO_2 air as the objective of this experiment was to determine the very early inflammatory response of surface modification after albumin adsorption using healthy cells in serum-free media [11]. The supernatant was collected and centrifuged to remove the cells and kept at −80 °C until further analysis. Secreted cytokines were measured by flow cytometry (BD Fortessa X-20) using the Multi-Plex Biolegend kit as per manufacturer's instructions.

2.10. Statistical analysis

All the experiments were conduct using three parallel samples and each experiment was repeated three times. GraphPad Prism (Graphpad, CA, USA) and OriginPro 8.5 (OriginLab Cooperation, USA) were used to draw graphs and perform statistical analysis. All results were presented as mean ± SEM. The effect of surface modifications was compared to smooth surface chemistry surface by using one-way analysis of variance (ANOVA). The level of significance (p-value) is denoted by using asterisk (*) where * = (<0.05), ** (<0.01), *** = (<0.001) and **** = (<0.0001).

3. Results

Model surfaces with desired hill-like nanotopographical and chemical properties were fabricated by immobilizing carboxyl acid group capped AuNPs of diameters of 16, 38, and 68 nm on a functional plasma polymer coating deposited from vapor of 2-methyl-2-oxazoline (pOX). These coatings are documented to retain a population of intact oxazoline rings which can be utilized for covalent surface binding of entities containing carboxyl acid groups such as proteins and nanoparticles [33]. An identical number of surface protrusions was achieved by adjusting the solution concentration and time of nanoparticles immobilization, as previously described [26].

3.1. Surface characterization

The surface morphology of the model substrata was characterized using AFM. Fig. 1a presents the 3D and 2D AFM images of the surface of pOX coated glass coverslip after plasma polymer layer deposition and immobilization of AuNPs. The 3D images demonstrate that the procedure resulted in hill-like nano-protrusions, whose height increased with the increase in nanoparticle size. This observation is also supported by the cross-sectional profiles presented in Fig. 1a. The 2D images show that the immobilization of nanoparticles created surface protrusions that have stochastic distribution with nearly complete absence of aggregations. The AFM images in Fig. 1a were utilized to calculate the number of nanoparticles per μm^2 to confirm that the number of surface protrusions were nearly identical on all surfaces. The results are presented in Fig. 1b and show that the number of immobilized nanoparticles on each nanotopography modified surface was 26 ± 1. The Root Mean Square roughness (RMS) was also calculated from the AFM images. As expected, the RMS increased with the increase in height of surface nanotopography from 3.5 < 10.3 < 16.2 nm (Fig. 1c). To generate uniform outermost surface chemistry, a 5 nm thin layer of pOX was deposited on top of the immobilized nanoparticles. This manner of surface engineering ensured that the only surface property that changed was the height of surface nanotopography while other parameters such as surface chemistry, nano-protrusions density, etc. remained the same for all model surfaces.

XPS was utilized to analyze the outermost surface chemistry of the modified surfaces (Fig. 1d). The pOX coating contained carbon (72 At%), nitrogen (12 At%), and oxygen (16 At%). After the immobilization of gold nanoparticles, an additional peak corresponding to Au 4f was detected demonstrating the successful addition of AuNPs (Fig. 1d). The intensity of the Au 4f peak increased with the increase in nanoparticles size (16 < 38< 68 nm). The deposition of an overcoating of pOX resulted in a decrease in the intensity of the Au 4f peak across all surfaces. This is expected taking into consideration the sampling depth of XPS. The wettability of the model surfaces was characterized by sessile drop water contact angle measurements. The results presented in Fig. 1e show that the increase in surface nanotopography feature size resulted in a decrease in the water contact angle which is consistent with Wenzel wetting state behaviour of hydrophilic surfaces [25].

3.2. Albumin adsorption

Albumin is the most abundant protein in the blood. It is also one of the first proteins that binds to foreign bodies constituting a significant fraction of the protein corona [34]. It is thus important to understand how biomaterial surface properties influence the amount and conformation of adsorbed albumin and how these may influence the subsequent immunological response. Human serum albumin adsorption on the model surface having well-defined surface topographical properties described above was measured by Micro BCA. Micro BCA is a colorimetric method in which protein acts as a catalyst for the conversion of cupric to cuprous ion resulting in the formation of purple color by bicinchoninic acid. Micro BCA (Fig. 2a) analysis showed that the amount of adsorbed HSA increased with an increase in the magnitude of surface roughness. The greater amount of adsorbed HSA could be directly related to the increase in the surface area caused by the addition of surface nanotopography (Fig. 2b).

3.3. Albumin unfolding

Conformational changes in the native form of albumin have been known to expose protein sequences that can then bind to the scavenger receptors of immune cells [15]. To determine the effect of surface nanotopography on the secondary structure of albumin, far UV-circular dichroism spectroscopy was performed using a modified method for studies on surfaces [5]. Fig. 3a shows the CDS spectrum of albumin in its native state. Two negative peaks at 220 nm and 208 nm are visible, which represent the $n \rightarrow \pi^*$ and $\pi \rightarrow \pi^*$ transitions of the α-helical secondary structure for albumin [35,36]. Fig. 3b illustrates the change in the secondary structure of albumin after adsorption onto modified surfaces with different nanotopography. Albumin on smooth pOX and 68 pOX exhibited the greatest change in $\alpha -$ helical structure as evidenced by the

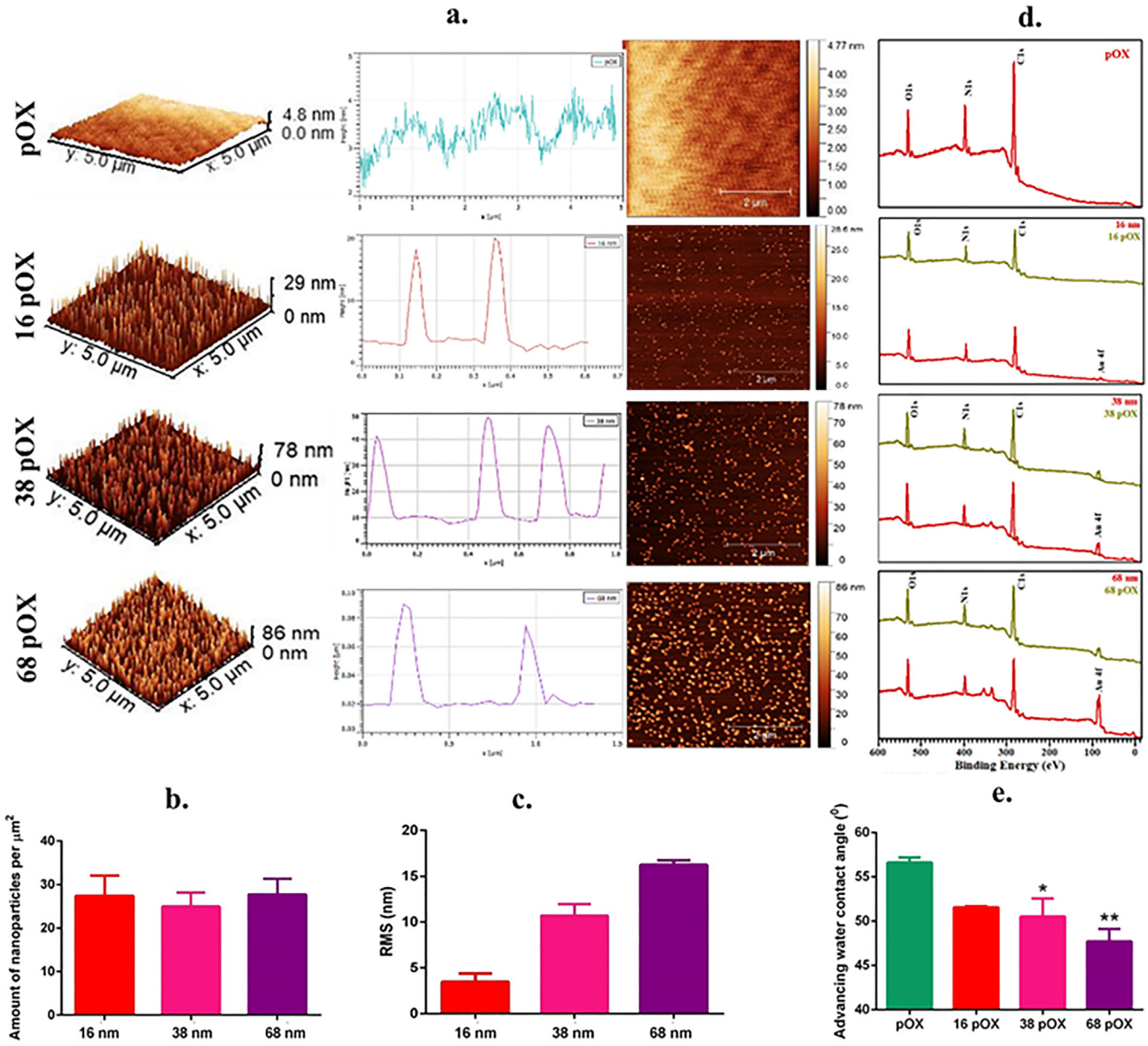

Fig. 1. Characterization of model substrata used in this study: (a) Atomic force microscope 3D and 2D images together with cross-sectional profiles of the surfaces of the model substrata after pOX (top) deposition and after immobilization of AuNPs having diameters of 16, 38 and 68 nm; (b) Number of nanoparticles per unit area of the surface calculated from the AFM images; (c) RMS values obtained from the AFM images; (d) XPS spectra of the model surfaces before and after overcoating with pOX, and (e) advancing water contact angle of the model surfaces (**e**).

reduction in ellipticity at 220 and 208 nm. However, the spectra of albumin on both 38 pOX and 16 pOX had minimal change in peaks negativity which can be attributed to less conformational change and better preservation of the secondary structure. The results obtained from CDS were then analysed using the Dicroweb software. Fig. 3c shows that native HSA possesses 63% of α-helices and 6% of β-sheets. Upon interaction with the surface, the α-helix structure of the protein was significantly altered on all surfaces suggesting significant conformational change of the molecule. The lowest retention of α-helix structure and greatest unfolding was noted on the smooth surface (pOX) and the surface having the greatest nanotopographical features (68 pOX).

3.4. Interaction of immune cells with modified surfaces

Studies of immune cell interaction with the nanotopography modified surfaces were performed using monocytes (THP-1) and macrophages (dTHP-1). Modified surfaces with and without pre-absorbed albumin were incubated with THP-1 cells for 1 h to determine cell adhesion. THP-1 cells adhered in very few numbers to any of these surfaces regardless of whether albumin was pre-adsorbed or not (Figure S1). This result was expected as these cells do not have adhesion receptors and albumin does not have the epitope for monocytes interaction [15]. Since there was no significant adhesion of monocytes with the modified surfaces, dTHP-1 cells were used for further immune cell studies. All surfaces with or without pre-adsorbed albumin showed significant adhesion of dTHP-1 cells. However, a significant reduction in the cell number

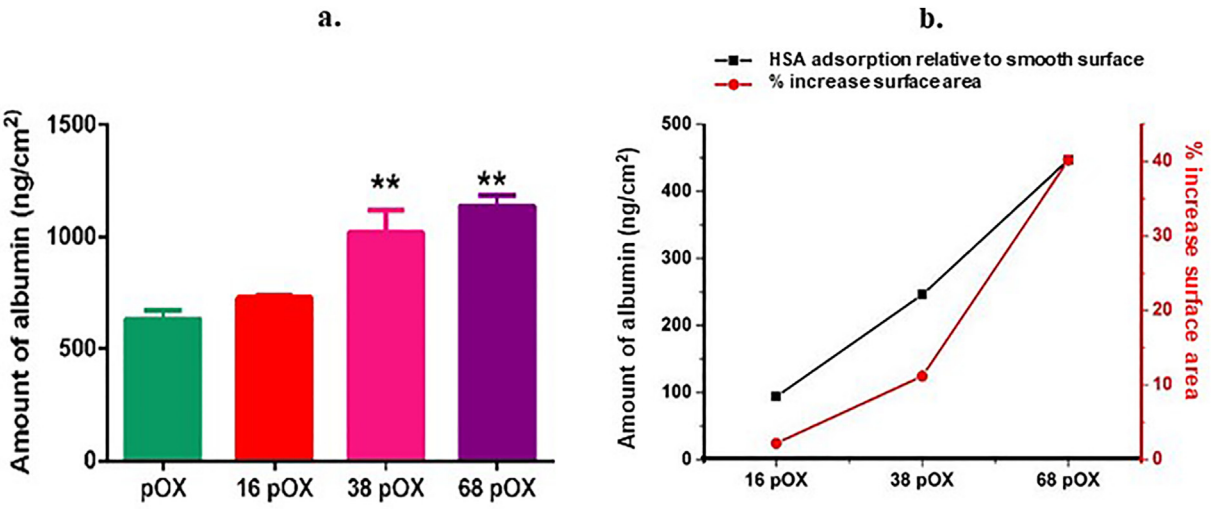

Fig. 2. (**a**) Human serum albumin adsorption on the surfaces with different topography obtained from Micro BCA. (**b**) Correlation between per cent increase surface area due to presence of nanotopography and increased amount of HSA.

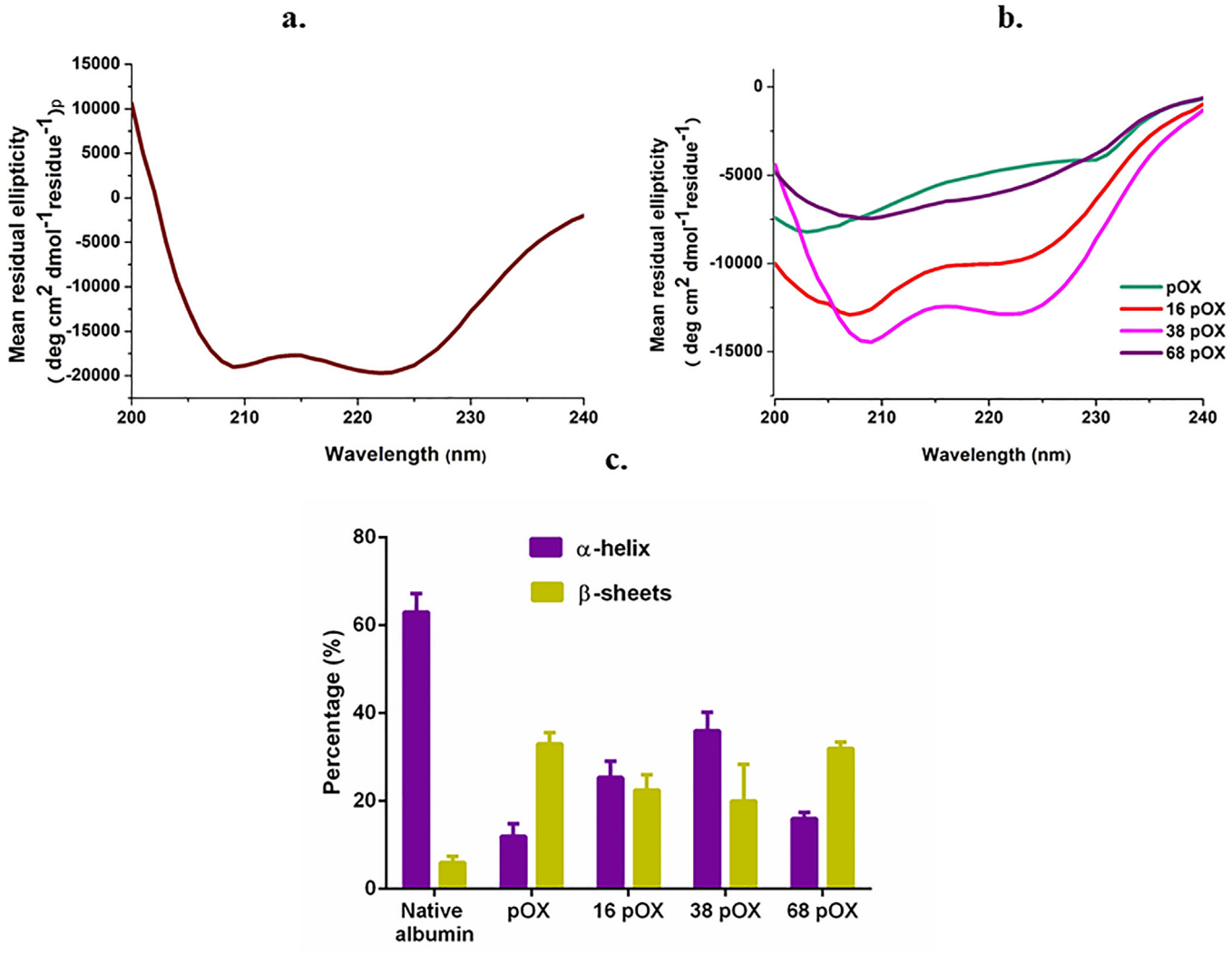

Fig. 3. Human serum albumin conformational changes upon adsorption on smooth pOX coated surface and surfaces with different topography. (a) CD spectrum of HSA (1 mg/mL) solution, (b) CD spectra of HSA adsorbed on the different model surfaces. (c) Percentage of α-helices and β-sheets present in HSA after adsorption on to the surfaces.

was observed on the surfaces having pre-adsorbed albumin (pOX-$p < 0.0001$; 16 pOX-$p < 0.01$; 38 pOX-$p < 0.001$; 68 pOX-$p < 0.0001$) compared to surfaces without (Fig. 4a). Furthermore, in the case of surfaces without pre-adsorbed albumin, no significant difference was observed in the number of adhered cells amongst the surfaces with different modifications (Fig. 4b). However, pre-adsorption of albumin resulted in a significant difference in cell numbers on 16 pOX, 38 pOX and 68 pOX ($p < 0.0001$) compared to pOX (Fig. 4c).

3.5. Selective binding of scavenger receptors (SR-A1) with albumin

To understand the mechanisms underpinning the reduction in number of macrophages on surfaces having pre-adsorbed albumin, we conducted further studies where certain pathways were blocked. Macrophages are known to interact with albumin using their scavenger receptors [15]. Therefore, we used polyionosinic acid (PI) which is known to act as a blocker for these receptors [37,38]. dTHP-1 cells were incubated with PI acid for 1 h to block the scavenger receptors and were then added to the modified surfaces with and without pre-adsorbed albumin.

When the scavenger receptors were blocked, the macrophages did not adhere to the albumin pre-coated surfaces ((HSA (+), PI (+)) (Blue color), whereas the same cells attached to surfaces without pre-adsorbed albumin ((HSA (−), PI (−)) (orange color) as no receptors were blocked (Fig. 5). However, cells with blocked scavenger receptors could adhere to the surfaces without pre-absorbed albumin ((HSA (−), PI (+)) (light green). This was possible since macrophages can still attach to the surface without albumin coating using other receptors such as the integrin receptors. With albumin pre-adsorbed, but the scavenger receptors not blocked ((HSA (+), PI (−)) (green), the cells still adhered to the surface although in smaller number than on (HSA (−), PI (−). These results support the data in Fig. 4 and confirm that albumin undergoes conformational change upon adsorption to the surface, thus presenting normally hidden peptide sequences, which in turn allows attachment of macrophages via the scavenger receptors.

3.6. Initial innate immune response

Monocytes (THP-1) and macrophages (dTHP-1) were incubated on the model surfaces with different nanotopography to determine inflammatory responses. After incubation, the supernatant was collected for analysis of pro- and anti-inflammatory cytokines expression. Negligeable cytokine expression was obtained from the monocytes and any difference amongst surfaces with different modifications was not statistically significant. This is expected as these cells are known to be non-surface adherent (Figure S2), discussed above.

Macrophages were incubated on the modified surfaces for 2 h and supernatant was collected for analysis. The expression of TNF-α was greater on 16 nm ($p < 0.001$), 38 nm ($p < 0.05$), and 68 nm ($p < 0.0001$) nanotopography modified surfaces compared to the smooth surfaces irrespective of albumin pre-adsorption (Fig. 6a and b). Amongst different nanotopography scales, the 38 nm caused the lowest levels of TNF-α while the 68 nm the greatest. However, an overall reduction in the expression of TNF-α expression was observed when surfaces had pre-adsorbed albumin (Fig. 6c). In order to gain insight at an individual cell level, the amount of expressed TNF-α normalized to the number of cells which had adhered to the surface. The result revealed that the reduction of TNF-α expression was significant only for the smallest nanotopography of 16 nm (Fig. 6d). In the case of IL-1β, a significant increase in the expression of this pro-inflammatory cytokine was observed on 68 nm nanotopography (Fig. 6e). There was no significant difference observed in IL-1β production amongst different surfaces when albumin was pre-adsorbed (Fig. 6f). Different from TNF-α, the only decrease in IL-1β expression on albumin pre-adsorbed surfaces was when the nanotopography scale was 16 nm and 68 nm, only the latter being statistically significant (Fig. 6g). Then considered at individual cell level, the expression of IL-1β was greater on albumin pre-adsorbed surfaces (although still lower that on samples without albumin), being statistically significant only in the case of pOX. (Fig. 6h). This supports the hypothesis that unfolding of albumin, most strongly observed on the smooth surface (pOX), can stimulate immune cells through exposure of normally hidden peptide sequences.

We also analysed the expression of anti-inflammatory cytokines IL-1RA and IL-10. There was no significant difference in the levels of expression of IL-1RA and IL-10 amongst the model surface with different nanotopography (Fig. 7a, b, e, and f). Overall, the expression of both IL-1RA and IL-10 were greater on the surfaces having pre-adsorbed albumin (Fig. 7c and g). The expression of IL-10 increased significantly on 16 pOX and 38 pOX ($p < 0.05$) surfaces having pre-adsorbed albumin compared to the analogous surfaces without. Further, we evaluated the expression of anti-inflammatory cytokines at individual cells level. These analyses revealed an increase in the secretion of IL-1RA on the pOX (<0.001) and 38 pOX (<0.05) surfaces (Fig. 7d). In the case of IL-10, the expression of this cytokine increased markedly on all surfaces having pre-adsorbed albumin except 68 pOX (Fig. 7h).

Collectively, the general trend pointed to a reduction of pro-inflammatory cytokines expression and an increase in anti-inflammatory cytokines production on surfaces containing pre-adsorbed albumin compared to analogous surfaces without

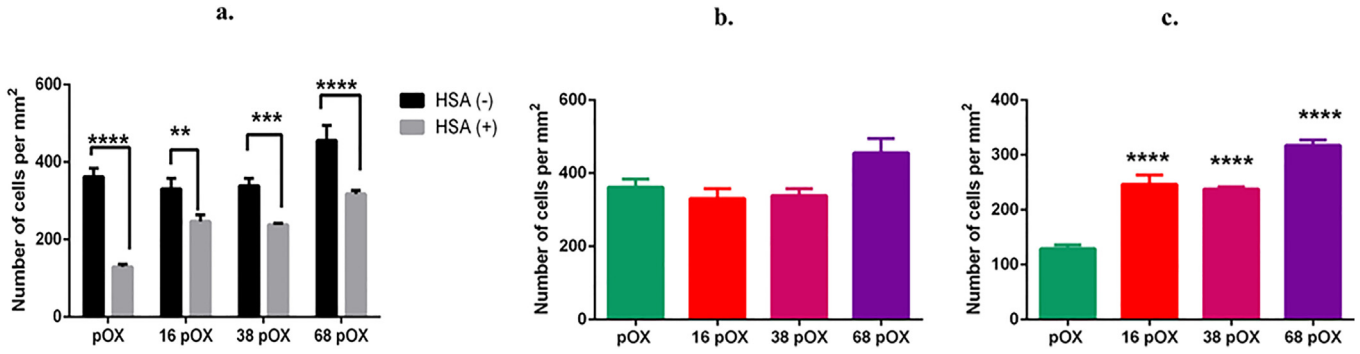

Fig. 4. Immune cell interaction. (a) The adhesion of macrophages (dTHP-1) with the model surfaces with and without pre-adsorbed albumin. b) The adhesion of macrophages on different model surfaces without pre-adsorbed HSA. (c) The adhesion of macrophages on to the different model surfaces with pre-adsorbed HSA. ($p < 0.01$**, 0.001*** and 0.0001****).

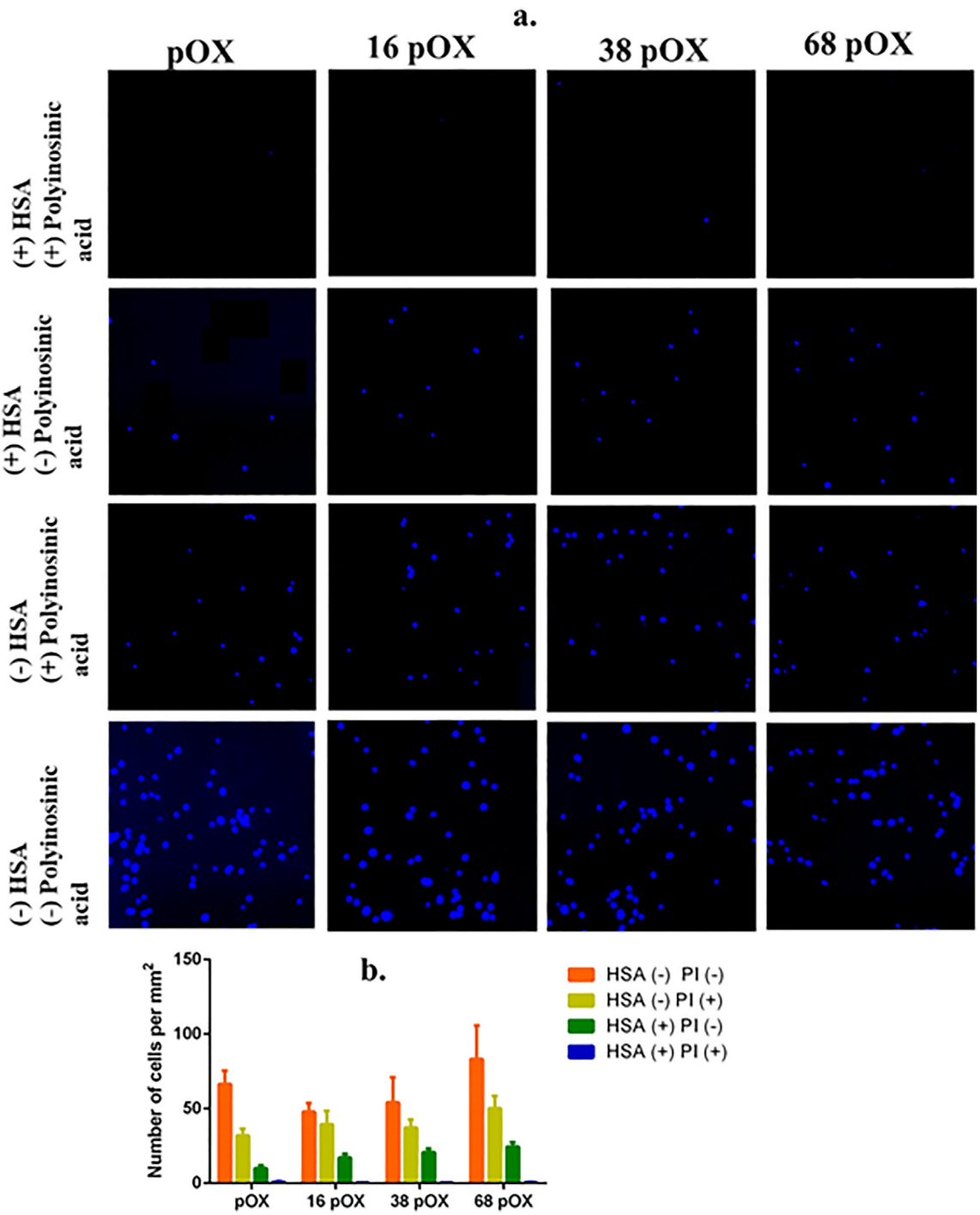

Fig. 5. (a) Fluorescence microscopy images and the (b) corresponding quantification of selective binding of dTHP-1 cells on the model surfaces having different topographical modification with and without scavenger receptor A1 blocker (polyinosinic acid), and pre-adsorption of albumin: without albumin and without PI ((HSA (−), PI (−)), without albumin and with PI ((HSA (−), PI (+)), with albumin and without PI ((HSA (+), PI (−)), and with albumin and with PI ((HSA (+), PI (+)).

albumin. Evaluation of the cytokine expression at individual cell level significantly enhanced this trend.

4. Discussion

Surface roughness plays an important role in promoting protein adsorption and modulating the subsequent inflammatory responses to biomaterials [9,11,12,39,40]. The introduction of nanoscale topography to the biomaterial surface can help mimic the extracellular matrix structure, which then imparts the capability to study the effect of surface roughness on biological responses *in vitro*. Proteins are known to spontaneously bind to the surface of biomaterials when in contact with biological fluids. The amount, orientation, and conformational changes of these proteins then govern the interaction with cellular receptors via different signaling pathways [9]. In this study, human serum albumin was utilized as it is an important small protein that is present in high amounts in the protein corona [34,41]. It is well known that albumin influences

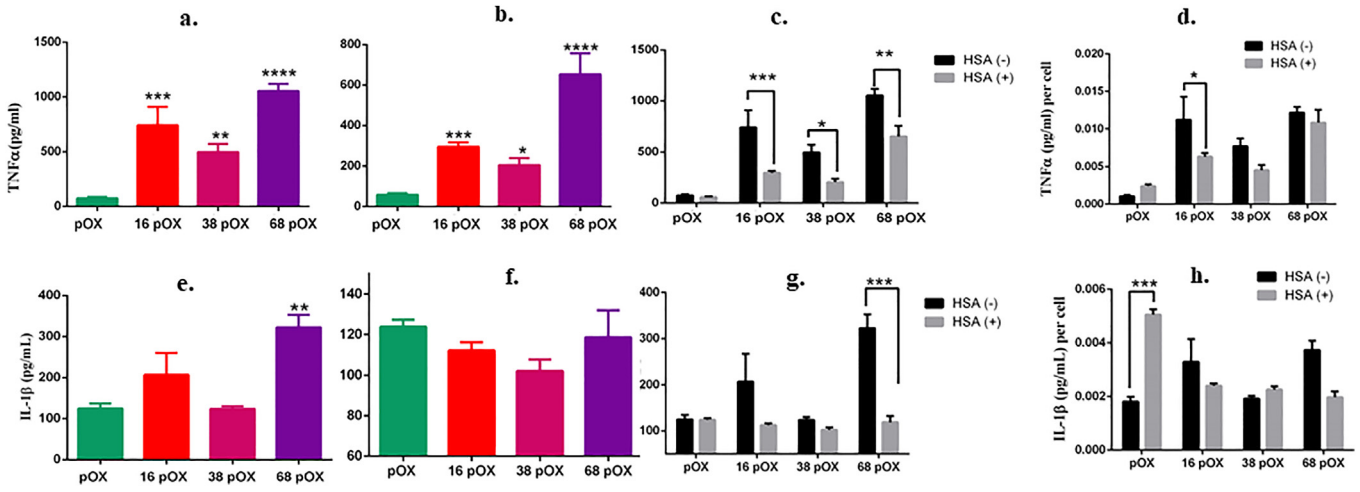

Fig. 6. Pro-inflammatory cytokines production from differentiated THP-1 (dTHP-1) cells on modified surfaces with and without pre-adsorbed human serum albumin. Secretion of TNF-α on surfaces without (a) and pre-adsorbed albumin (b). Comparison of TNF-α expression on surface with and without pre-adsorbed HSA (c). Comparison of TNF-α expression per cell (d) Secretion of IL-1β on surfaces without (e) and with pre-adsorbed albumin (f). Comparison of IL-1β expression on surface with and without HSA (g). Comparison of IL-1β expression per cell (h) $p < 0.05$ *, 0.01**, 0.001***, 0.0001****.

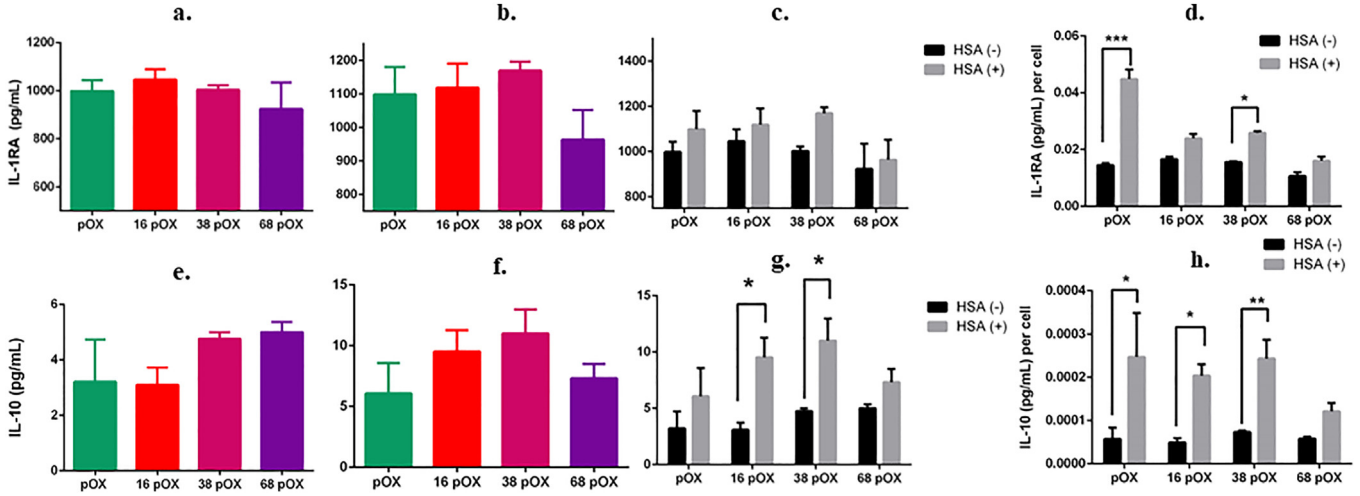

Fig. 7. Anti-inflammatory cytokines production from dTHP-1 cells on the modified surfaces with and without pre-adsorbed human serum albumin. Expression of IL-1RA on surfaces without albumin (a) and with pre-adsorbed albumin (b). Comparison of IL-1RA expression on surface with and without HSA (c). Comparison of IL-1RA expression per cell (d). Expression of IL-10 on surfaces without albumin (e) and pre-adsorbed albumin (f). Comparison IL-10 expression on surface with and without HSA (g). Comparison of IL-10 expression per cell (h). $p < 0.05$ *, 0.01**, 0.001***.

nanoparticle clearance by interacting with the surface receptors of immune cells [15,42]. However, a gap in knowledge still exists regarding the influence of adsorbed albumin on cellular responses following biomaterial implantation. Thus, the purpose of this work was, via generating model biomaterial substrata, to shed light on the affect if surface nanotopographical modification on the modulation of albumin binding, unfolding, and the subsequent immune responses.

To test our hypothesis, model substrata were fabricated by utilizing our well-established protocols, where AuNPs having well controlled sizes of 16, 38, and 68 nm are covalently immobilized to a pOX plasma polymer layer [26]. This type of surface modification, where the only parameter that changes is the surface nanohill-like dimensions, opens possibilities to study the effect of pure surface nanotopography on various biological responses. AFM imaging confirmed an increase in surface roughness with the increase in the diameter of AuNPs [43] (Fig. 1a). Chemical analysis by XPS confirmed the identical outermost surface chemical composition of all surfaces. Along with surface roughness, the surface wettability of the modified surface was also altered. Advancing water contact angle of the nanoparticles modified surfaces decreased with increasing surface roughness (Fig. 1e) and points to a Wenzel wetting state [25].

Surfaces modified in this manner were then utilized to explore albumin adsorption and unfolding. Surface protein adsorption is dependent on many factors such as concentration, diffusion coefficient, size of the protein, affinity to the material, electrical double layer, and London interaction between protein particles and the surfaces [44,45]. Introducing nanotopography to these surfaces increased the surface roughness, hence, the surface area available for protein adsorption [45]. Elter et al. described how proteins accumulate on rough surfaces compared to planar surfaces. These workers used nanogrooves with convex and concave corners to explain this phenomenon. They determined that initially, protein

molecules interact with convex edges due to high electrostatic forces. Later, proteins migrate towards concave edges by high dispersion interactions [44]. In our study, albumin adsorption increased with the increase in surface roughness (Fig. 2a). The increase in adsorbed protein amount followed the same trend as the increase in the surface area associated with greater nanotopography features (Fig. 2b).

We also found that adsorbed albumin undergoes conformational changes on our model surfaces regardless of the presence of surface nanotopography and its scale (Fig. 3). These conformational changes included a reduction in the protein α-helicity and an increase in the number of β-sheets compared to native albumin. Numerous studies have been performed to determine the conformational change of proteins upon adsorption [5,15,46–52]. Picó has explored unfolding of albumin through three processes (native ↔ unfolded reversible ↔ unfolded irreversible) when increasing the temperature [51]. Dockal et al. found that albumin structural transition is pH-dependent and can undergo tertiary structure isomerization at alkaline pH. Furthermore, domain II was more susceptible to loosening its structure at acidic pH [46]. The structure of albumin after adsorption onto silica particles has altered and the structural changes were dependent on the buffer used [48]. The changing of structure is also dependent on the nanoparticle concentration [15]. The surface chemistry of biomaterials is known to affects the adsorption and unfolding of albumin [5,49]. In this study, we focused on the role of surface nanotopography. The temperature, buffer, density of nanoprotrusions and pH were kept constant while the only parameter that changed was surface nanotopography. We found that albumin undergoes the greatest structural change on smooth pOX surface and the nanotopography of highest scale (68 nm) while fewer conformational changes were observed on the smaller topographic features.

The importance of immune cells response to surfaces with adsorbed albumin is well recognized [53]. Therefore, we further studied how albumin adsorption and conformational change on our model substrates affect the very initial immune cell responses. Protein adsorption onto a biomaterial surface mediates the interaction with immune cells through specific receptors for specific proteins. Albumin is recognized by the scavenger receptor-A (SR-A1) of macrophages, which in the case of small particles, facilitates cellular uptake [15,54,55]. SR-AI macrophage scavenger receptors are type II surface glycoproteins (~220 kDa) comprised of structurally identical three subunits. Each subunit is composed of several domains: intracellular *N*-terminal domain, a transmembrane region, a spacer domain, an α-helical coiled-coil domain, collagenous domain, and *C*-terminal isoform-specific domain. The *C*-terminal isoform-specific domain has cysteine-containing tandem repeats [56]. SR-A1 receptors mainly bind with polyanionic ligands via electrostatic interaction through its charged segments present in the collagenous region [56]. The positively charged regions of SR-A1 bind with albumin polyanionic regions present in domain I and domain II [15]. The binding of monocytes on our modified model surfaces, both, with and without pre-adsorbed albumin, was negligible (<25 cells/mm^2-Figure S1) due to the absence of receptors for interaction. However, macrophages (dTHP-1) bound to both surfaces (with and without albumin pre adsorption) but in fewer numbers on these with pre-adsorbed albumin since binding occurred only due to the interaction through only SR-A1 [15]. Blocking of the scavenger receptor with polyionosinic acid demonstrated that this is indeed the binding pathway to the surfaces having pre-adsorbed albumin. Our surfaces induce conformational change of albumin domain 1 or/and II which facilitates interaction with the cationic regions of SR-A1 by electrostatic interactions. (Scheme 4).

Important for application on biomaterial surfaces, we further examined the expression of pro- and anti-inflammatory cytokines on the model surfaces as a measure of the initial innate immune response. Overall, there was no notable influence of the scale of surface nanotopography on pro-inflammatory cytokine expression, surfaces with pre-adsorbed albumin led to reduction in the expression of TNF-α and IL-1β compared to analogous surfaces without albumin. The results retained broadly the same trend at an individual cell level. An exception was the smooth surface where the opposite effect was observed i.e., IL-1β expression significantly

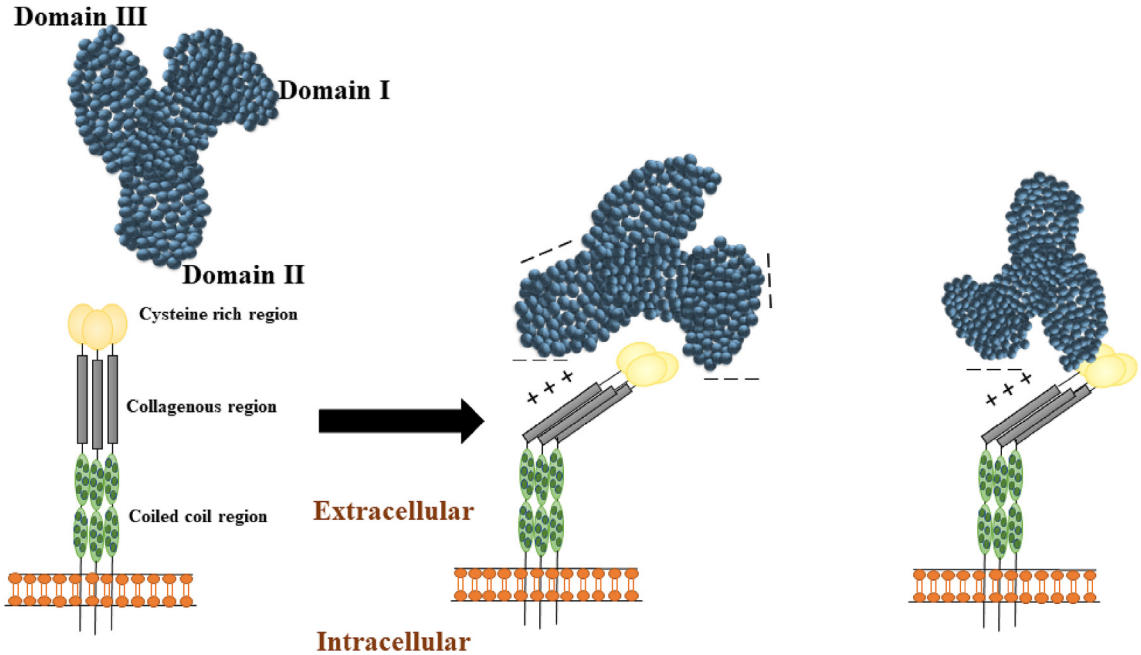

Scheme 4. Schematic representation of the interaction between albumin and scavenger receptor A1. Cationic sections of the collagenous region can bind with the polyanionic regions of conformationally changed domain I and domain II of albumin [56,57].

increased on the surface having pre-adsorbed albumin, the latter being attributable to the high level of albumin unfolding on this type of surface. The expression of anti-inflammatory cytokines significantly increased after albumin pre-adsorption on the surface. This is consistent with the work of Mijiritsky et al. who investigated the influence of albumin-impregnated bone granules on immune cells and stem cells. They showed albumin-impregnated bones increased the secretion of IL-10 over time compared to control bone [41]. In our study, all surfaces showed increase in the production of IL-1RA and IL-10 compared to analogues without albumin, the least being on highest nanotopography (68 pOX). These results indicate that pre-adsorption of albumin on biomaterial surfaces may induce macrophage toward the anti-inflammatory pathways.

5. Conclusions

This study examines the role of surface nanotopography on albumin adsorption, unfolding and the subsequent inflammatory response. We create model surfaces of hill-like nanoprotrusions by covalently immobilizing AuNPs of predetermined sizes (16, 38, and 68 nm) on the plasma polymerized pOX layer. A thin (5 nm), continuous and pinhole-free layer of pOX was then applied to tailor the outermost chemistry while preserving the scale of surface nanotopography. The amount of adsorbed albumin increased with the magnitude of surface nanotopography features, which could be explained with the greater surface area. CDS studies pointed to conformational changes in albumin upon adsorption to all surface with most significant loss of α-helix structure on the smooth surface and this with greatest nanotopography (68 nm). Studies with differentiated THP-1 cells demonstrated that macrophages interact with the surfaces through the scavenger SR-AI receptors. Pre-adsorption of albumin resulted in an overall decrease in the level of expression of pro-inflammatory cytokines. On the other hand, pre-adsorption of albumin resulted in an increase in the production of anti-inflammatory markers, which suggests the inflammatory response directs towards anti-inflammatory wound healing pathway. The knowledge obtained from this study can instruct the design of healthcare materials where generation of targeted surface nanotopography and pre-adsorption of albumin may enhance the biomaterial biocompatibility and lead to accelerated healing.

Credit author statement

Panthihage Ruvini Lakshika Dabare: Conceptualization, Methodology, Investigation (carried out experiments and data collection), Formal analysis, Writing – original draft, Visualization, Project administration. Akash Bachhuka: Methodology, Formal analysis, Writing – review & editing. Emma Parkinson-Lawrence: Methodology, Formal analysis, Providing resources, Writing – review & editing. Krasimir Vasilev: Supervision, Conceptualization, Methodology, Providing resources, Writing – review & editing, Project administration, Funding acquisition.

Funding

KV thanks NHMRC, Australia for Fellowship GNT1194466 and Australian Research Council (ARC) for grant DP180101254. AB thanks MICINN (Spain) for Juan de la Cierva incorporation fellowship IJC-2019-042374-1.

Declaration of competing interest

The authors declare that they have no known competing financial interests or personal relationships that could have appeared to influence the work reported in this paper.

Acknowledgements

We thank to Microscopic Australia Technical service for facilitating required instrument and services for imaging. (Authors 1 and 2 contributed equally to this work).

Appendix A. Supplementary data

Supplementary data to this article can be found online at https://doi.org/10.1016/j.mtadv.2021.100187.

References

[1] J.M. Anderson, A. Rodriguez, D.T. Chang, Foreign body reaction to biomaterials, Semin. Immunol. 20 (2008) 86–100, https://doi.org/10.1016/j.smim.2007.11.004.
[2] D.D. Deligianni, N. Katsala, S. Ladas, D. Sotiropoulou, J. Amedee, Y.F. Missirlis, Effect of surface roughness of the titanium alloy Ti-6Al-4V on human bone marrow cell response and on protein adsorption, Biomaterials 22 (2001) 1241–1251, https://doi.org/10.1016/S0142-9612(00)00274-X.
[3] Z. Adamczyk, M. Nattich-Rak, M. Dąbkowska, M. Kujda-Kruk, Albumin adsorption at solid substrates: a quest for a unified approach, J. Colloid Interface Sci. 514 (2018) 769–790, https://doi.org/10.1016/j.jcis.2017.11.083.
[4] S.N. Christo, K.R. Diener, A. Bachhuka, K. Vasilev, J.D. Hayball, Innate immunity and biomaterials at the nexus: friends or foes, BioMed Res. Int. (2015) 2015, https://doi.org/10.1155/2015/342304.
[5] B. Sivaraman, R.A. Latour, The Adherence of platelets to adsorbed albumin by receptor-mediated recognition of binding sites exposed by adsorption-induced unfolding, Biomaterials 31 (2010) 1036–1044, https://doi.org/10.1016/j.biomaterials.2009.10.017.
[6] Z.J. Deng, M. Liang, I. Toth, M. Monteiro, R.F. Minchin, Plasma protein binding of positively and negatively charged polymer-coated gold nanoparticles elicits different biological responses, Nanotoxicology 7 (2013) 314–322, https://doi.org/10.3109/17435390.2012.655342.
[7] L.E. Gonzalez Garcia, M. MacGregor-Ramiasa, R.M. Visalakshan, K. Vasilev, Protein interactions with nanoengineered polyoxazoline surfaces generated via plasma deposition, Langmuir 33 (2017) 7322–7331, https://doi.org/10.1021/acs.langmuir.7b01279.
[8] T. Khampieng, V. Yamassatien, P. Ekabutr, P. Pavasant, P. Supaphol, Protein adsorption and cell behaviors on polycaprolactone film: the effect of surface topography, Adv. Polym. Technol. 37 (2018) 2030–2042, https://doi.org/10.1002/adv.21861.
[9] M.S. Lord, M. Foss, F. Besenbacher, Influence of nanoscale surface topography on protein adsorption and cellular response, Nano Today 5 (2010) 66–78, https://doi.org/10.1016/j.nantod.2010.01.001.
[10] D. Fabrizius-Homan, S. Cooper, A comparison of the adsorption of three adhesive proteins to biomaterial surfaces, J. Biomater. Sci. Polym. Ed. 3 (1992) 27–47, https://doi.org/10.1163/156856292X00060.
[11] R.M. Visalakshan, A.A. Cavallaro, M.N. MacGregor, E.P. Lawrence, K. Koynov, J.D. Hayball, K. Vasilev, Nanotopography-Induced Unfolding of Fibrinogen Modulates Leukocyte Binding and Activation, Advanced Functional Materials, 2019, https://doi.org/10.1002/adfm.201807453.
[12] M. Shen, T.A. Horbett, The effects of surface chemistry and adsorbed proteins on monocyte/macrophage adhesion to chemically modified polystyrene surfaces, J. Biomed. Mater. Res. 57 (2001) 336–345, https://doi.org/10.1002/1097-4636(20011205)57:3%3C336::AID-JBM1176%3E3.0.CO;2-E.
[13] B.G. Keselowsky, A.W. Bridges, K.L. Burns, C.C. Tate, J.E. Babensee, M.C. LaPlaca, A.J. Garcia, Role of plasma fibronectin in the foreign body response to biomaterials, Biomaterials 28 (2007) 3626–3631, https://doi.org/10.1016/j.biomaterials.2007.04.035.
[14] I.E. Svendsen, O. Santos, J. Sotres, A. Wennerberg, K. Breding, T. Arnebrant, L. Lindh, Adsorption of HSA, IgG and laminin-1 on model hydroxyapatite surfaces—effects of surface characteristics, Biofouling 28 (2012) 87–97, https://doi.org/10.1080/08927014.2011.653562.
[15] G.M. Mortimer, N.J. Butcher, A.W. Musumeci, Z.J. Deng, D.J. Martin, R.F. Minchin, Cryptic epitopes of albumin determine mononuclear phagocyte system clearance of nanomaterials, ACS Nano 8 (2014) 3357–3366, https://doi.org/10.1021/nn405830g.
[16] M.E. Sitar, S. Aydin, U. Cakatay, Human serum albumin and its relation with oxidative stress, Clin. Lab. 59 (2013) 945–952.
[17] P. Lee, X. Wu, Modifications of human serum albumin and their binding effect, Curr. Pharmaceut. Des. 21 (2015) 1862–1865.
[18] E.C. Reynolds, A. Wong, Effect of adsorbed protein on hydroxyapatite zeta potential and Streptococcus mutans adherence, Infect. Immun. 39 (1983) 1285–1290, https://doi.org/10.1128/iai.39.3.1285-1290.1983.
[19] K. Kottke-Marchant, J.M. Anderson, Y. Umemura, R.E. Marchant, Effect of albumin coating on the in vitro blood compatibility of Dacron® arterial prostheses, Biomaterials 10 (1989) 147–155, https://doi.org/10.1016/0142-9612(89)90017-3.
[20] M. Amiji, K. Park, Surface modification of polymeric biomaterials with poly(ethylene oxide), albumin, and heparin for reduced thrombogenicity,

J. Biomater. Sci. Polym. Ed. 4 (1993) 217–234, https://doi.org/10.1163/156856293X00537.
[21] Y. An, G. Stuart, S. McDowell, S. McDaniel, Q. Kang, R. Friedman, Prevention of bacterial adherence to implant surfaces with a crosslinked albumin coating in vitro, J. Orthop. Res. 14 (1996) 846–849, https://doi.org/10.1002/jor.1100140526.
[22] J. Mariam, S. Sivakami, P.M. Dongre, Albumin corona on nanoparticles–a strategic approach in drug delivery, Drug Deliv. 23 (2016) 2668–2676, https://doi.org/10.3109/10717544.2015.1048488.
[23] S.N. dos Santos, S.R. Rezende Dos Reis, L.P. Pires, E. Helal-Neto, F. Sancenón, T.C. Barja-Fidalgo, R. Medina de Mattos, L.E. Nasciutti, R. Martínez-Máñez, R. Santos-Oliveira, Avoiding the mononuclear phagocyte system using human albumin for mesoporous silica nanoparticle system, Microporous Mesoporous Mater. 251 (2017) 181–189, https://doi.org/10.1016/j.micromeso.2017.06.005.
[24] M. Holmberg, X. Hou, Competitive protein adsorption of albumin and immunoglobulin G from human serum onto polymer surfaces, Langmuir 26 (2010) 938–942, https://doi.org/10.1021/la902409n.
[25] M. Ramiasa-MacGregor, A. Mierczynska, R. Sedev, K. Vasilev, Tuning and predicting the wetting of nanoengineered material surface, Nanoscale 8 (2016) 4635–4642, https://doi.org/10.1039/c5nr08329j.
[26] R.M. Visalakshan, M.N. MacGregor, A.A. Cavallaro, S. Sasidharan, A. Bachhuka, A.M. Mierczynska-Vasilev, J.D. Hayball, K. Vasilev, Creating nano-engineered biomaterials with well-defined surface descriptors, ACS Appl. Nano Mat. 1 (2018) 2796–2807, https://doi.org/10.1021/acsanm.8b00458.
[27] T. Zhu, K. Vasilev, M. Kreiter, S. Mittler, W. Knoll, Surface modification of citrate-reduced colloidal gold nanoparticles with 2-mercaptosuccinic acid, Langmuir 19 (2003) 9518–9525, https://doi.org/10.1021/la035157u.
[28] D. Nečas, P. Klapetek, Gwyddion: an open-source software for SPM data analysis, Open Phys. 10 (2012) 181–188, https://doi.org/10.2478/s11534-011-0096-2.
[29] L. Whitmore, B. Wallace, DICHROWEB, an online server for protein secondary structure analyses from circular dichroism spectroscopic data, Nucleic Acids Res. 32 (2004) W668–W673, https://doi.org/10.1093/nar/gkh371.
[30] L. Whitmore, B.A. Wallace, Protein secondary structure analyses from circular dichroism spectroscopy: methods and reference databases, Biopolymers: Original Res. Biomo. 89 (2008) 392–400, https://doi.org/10.1002/bip.20853.
[31] M. Andrade, P. Chacon, J. Merelo, F. Morán, Evaluation of secondary structure of proteins from UV circular dichroism spectra using an unsupervised learning neural network, Protein Eng. Des. Sel. 6 (1993) 383–390, https://doi.org/10.1093/protein/6.4.383.
[32] R.M. Visalakshan, M.N. MacGregor, S. Sasidharan, A. Ghazaryan, A.M. Mierczynska-Vasilev, S. Morsbach, V. Mailander, K. Landfester, J.D. Hayball, K. Vasilev, Biomaterial surface hydrophobicity-mediated serum protein adsorption and immune responses, ACS Appl. Mater. Interfaces 11 (2019) 27615–27623, https://doi.org/10.1021/acsami.9b09900.
[33] M. Ramiasa, A. Cavallaro, A. Mierczynska, S. Christo, J. Gleadle, J. Hayball, K. Vasilev, Plasma polymerised polyoxazoline thin films for biomedical applications, Chem. Commun. 51 (2015) 4279–4282, https://doi.org/10.1039/C5CC00260E.
[34] V. Serpooshan, M. Mahmoudi, M. Zhao, K. Wei, S. Sivanesan, K. Motamedchaboki, A.V. Malkovskiy, A.B. Goldstone, J.E. Cohen, P.C. Yang, Protein corona influences cell–biomaterial interactions in nanostructured tissue engineering scaffolds, Adv. Funct. Mater. 25 (2015) 4379–4389, https://doi.org/10.1002/adfm.201500875.
[35] S. Kumar, P. Kukutla, N. Devunuri, P. Venkatesu, How does cholinium cation surpass tetraethylammonium cation in amino acid-based ionic liquids for thermal and structural stability of serum albumins? Int. J. Biol. Macromol. 148 (2020) 615–626, https://doi.org/10.1016/j.ijbiomac.2020.01.135.
[36] Y. Wei, A.A. Thyparambil, R.A. Latour, Protein helical structure determination using CD spectroscopy for solutions with strong background absorbance from 190 to 230 nm, Biochim. Biophys. Acta 1844 (2014) 2331–2337, https://doi.org/10.1016/j.bbapap.2014.10.001.
[37] M.E. Haberland, A.M. Fogelman, Scavenger receptor-mediated recognition of maleyl bovine plasma albumin and the demaleylated protein in human monocyte macrophages, Proc. Natl. Acad. Sci. Unit. States Am. 82 (1985) 2693–2697, https://doi.org/10.1073/pnas.82.9.2693.
[38] C.J. Obot, M.T. Morandi, T.P. Beebe Jr., R.F. Hamilton, A. Holian, Surface components of airborne particulate matter induce macrophage apoptosis through scavenger receptors, Toxicol. Appl. Pharmacol. 184 (2002) 98–106, https://doi.org/10.1006/taap.2002.9493.
[39] C.R. Jenney, J.M. Anderson, Adsorbed serum proteins responsible for surface dependent human macrophage behavior, J. Biomed. Mater. Res. 49 (2000) 435–447, https://doi.org/10.1002/(SICI)1097-4636(20000315)49:4%3C435::AID-JBM2%3E3.0.CO;2-Y.
[40] E. Westas Janco, M. Hulander, M. Andersson, Curvature-dependent effects of nanotopography on classical immune complement activation, Acta Biomater. 74 (2018) 112–120, https://doi.org/10.1016/j.actbio.2018.04.053.
[41] E. Mijiritsky, C. Gardin, L. Ferroni, Z. Lacza, B. Zavan, Albumin-impregnated bone granules modulate the interactions between mesenchymal stem cells and monocytes under in vitro inflammatory conditions, Mater. Sci. Eng. C 110 (2020) 110678, https://doi.org/10.1016/j.msec.2020.110678.
[42] M. Ahmed, R. Baumgartner, S. Aldi, P. Dusart, U. Hedin, B. Gustafsson, K. Caidahl, Human serum albumin-based probes for molecular targeting of macrophage scavenger receptors, Int. J. Nanomed. 14 (2019) 3723–3741, https://doi.org/10.2147/IJN.S197990.
[43] Z. Chen, A. Bachhuka, S. Han, F. Wei, S. Lu, R.M. Visalakshan, K. Vasilev, Y. Xiao, Tuning chemistry and topography of nanoengineered surfaces to manipulate immune response for bone regeneration applications, ACS Nano 11 (2017) 4494–4506, https://doi.org/10.1021/acsnano.6b07808.
[44] P. Elter, R. Lange, U. Beck, Electrostatic and dispersion interactions during protein adsorption on topographic nanostructures, Langmuir 27 (2011) 8767–8775, https://doi.org/10.1021/la201358c.
[45] D.A. Puleo, Rena Bizios, Biological Interactions on Materials Surfaces: Understanding and Controlling Protein, Cell, and Tissue Responses, Springer Science & Business Media, 2009.
[46] M. Dockal, D.C. Carter, F. Rüker, Conformational transitions of the three recombinant domains of human serum albumin depending on pH, J. Biol. Chem. 275 (2000) 3042–3050, https://doi.org/10.1074/jbc.275.5.3042.
[47] N.J. Greenfield, Using circular dichroism spectra to estimate protein secondary structure, Nat. Protoc. 1 (2006) 2876–2890, https://doi.org/10.1038/nprot.2006.202.
[48] H. Larsericsdotter, S. Oscarsson, J. Buijs, Structure, stability, and orientation of BSA adsorbed to silica, J. Colloid Interface Sci. 289 (2005) 26–35, https://doi.org/10.1016/j.jcis.2005.03.064.
[49] P. Roach, D. Farrar, C.C. Perry, Interpretation of protein adsorption: surface-induced conformational changes, J. Am. Chem. Soc. 127 (2005) 8168–8173, https://doi.org/10.1021/ja042898o.
[50] N. Li, Y. Zhang, B. Huang, H. Li, Ultrasonic dispersion temperature- and pH-tuned spectral and electrochemical properties of bovine serum albumin on carbon nanotubes and its conformational transition, Electrochim. Acta 296 (2019) 555–564, https://doi.org/10.1016/j.electacta.2018.11.089.
[51] G.A. Picó, Thermodynamic features of the thermal unfolding of human serum albumin, Int. J. Biol. Macromol. 20 (1997) 63–73, https://doi.org/10.1016/S0141-8130(96)01153-1.
[52] V. Hlady, Jos Buijs, Protein adsorption on solid surfaces, Curr. Opin. Biotechnol. 7 (1996) 72–77, https://doi.org/10.1016/S0958-1669(96)80098-X.
[53] M. Werthén, A. Sellborn, M. Källtorp, H. Elwing, P. Thomsen, In vitro study of monocyte viability during the initial adhesion to albumin- and fibrinogen-coated surfaces, Biomaterials 22 (2001) 827–832, https://doi.org/10.1016/S0142-9612(00)00246-5.
[54] R. Cai, C. Chen, The crown and the scepter: roles of the protein corona in nanomedicine, Adv. Mater. (2018), e1805740, https://doi.org/10.1002/adma.201805740.
[55] Y. Yan, K.T. Gause, M.M.J. Kamphuis, C.-S. Ang, N.M. O'Brien-Simpson, J.C. Lenzo, E.C. Reynolds, E.C. Nice, F. Caruso, Differential roles ofthe protein corona in the cellular uptake of nanoporous polymer particles by monocyte and macrophage cell lines, ACS Nano 7 (2013) 10960–10970, https://doi.org/10.1021/nn404481f.
[56] V.G. Martínez, S.K. Moestrup, U. Holmskov, J. Mollenhauer, F. Lozano, The conserved scavenger receptor cysteine-rich superfamily in therapy and diagnosis, Pharmacol. Rev. 63 (2011) 967–1000.
[57] N. Platt, S. Gordon, Is the class A macrophage scavenger receptor (SR-A) multifunctional?—the mouse's tale, J. Clin. Invest. 108 (2001) 649–654.